Inorg. Chem. **2005**, *44*, 5580–5590

Structure and Conformation of Bis(acetylacetonato)oxovanadium(IV) and Bis(maltolato)oxovanadium(IV) in Solution Determined by Electron Nuclear Double Resonance Spectroscopy

Devkumar Mustafi and Marvin W. Makinen*

Department of Biochemistry and Molecular Biology, Center for Integrative Science, The University of Chicago, 929 East 57th Street, Chicago, Illinois 60637

Received November 3, 2004

The structure and conformation of bis(acetylacetonato)oxovanadium(IV) [$VO(acac)_2$] and bis(maltolato)oxovanadium(IV) [$VO(malto)_2$] in frozen methanol have been determined by application of electron nuclear double resonance (ENDOR) spectroscopy. The positions of inner- and outer-sphere-coordinated solvent were assigned by ENDOR through use of selectively deuterated analogues of methanol. Similarly, the methyl and methylinyl proton resonance features of $VO(acac)_2$ were identified by site-selective deuteration. For $VO(acac)_2$, the ENDOR-determined metal–proton distances were best accounted for by a complex of tetragonal-pyramidal geometry, essentially identical to that determined by X-ray crystallography [Dodge, R. P.; Templeton, D. H.; Zalkin, A. *J. Chem. Phys.* **1961**, *35*, 55] but with an inner-sphere solvent molecule coordinated *trans* to the vanadyl oxygen and an axially positioned solvent molecule hydrogen-bonded to the vanadyl oxygen. In contrast to its *trans* conformation in crystals [Caravan, P.; et al. *J. Am. Chem. Soc.* **1995**, *117*, 12759], the $VO(malto)_2$ complex was found in a *cis* conformation whereby the donor oxygen atoms of one maltolato ligand occupied equatorial coordination sites. One of the donor oxygen atoms of the second maltolato ligand occupied the axial coordination site opposite the vanadyl oxygen atom, and the other an equatorial position. An inner-sphere-coordinated methanol molecule in the equatorial plane and a solvent molecule hydrogen-bonded to the vanadyl oxygen were also identified. No evidence for the *trans* isomer was observed.

Introduction

The insulin-enhancing properties of VO^{2+} and of VO^{2+} chelates in diabetic laboratory animals[1] and humans[2] have commanded widespread scientific attention because of the potential for improved therapy through drug design. Although the molecular basis is not known, it is established that the insulin-mimetic action of VO^{2+} chelates, measured as lowering of serum glucose levels in animals[1] or as glucose uptake[3] or lipogenesis[4] in adipocytes, greatly exceeds that of inorganic VO^{2+}. Recent studies from our laboratory demonstrate that bis(acetylacetonato)oxovanadium(IV) [$VO(acac)_2$; see ref 5 for abbreviations] potentiates the tyrosine phosphorylation activity of the insulin receptor and synthesis of glycogen in 3T3-L1 adipocytes.[3b] Inorganic VO^{2+} and $VO(malto)_2$ are also known to exhibit insulin-like activity;[1,2] however, we have not found them to act synergistically with insulin, in contrast to $VO(acac)_2$.[3b] The insulin-like activity of inorganic VO^{2+} has been shown to occur through an insulin-independent pathway,[6a] and the insulin-like action of $VO(malto)_2$ has been ascribed to reversible inhibition of protein tyrosine phosphatases by the

* To whom correspondence should be addressed. E-mail: makinen@uchicago.edu.

(1) (a) McNeill, J. H.; Yuen, V. G.; Hoveyda, H. R.; Orvig, C. *J. Med. Chem.* **1992**, *35*, 1489. (b) Yuen, V. G.; Orvig, C.; McNeill, J. H. *Can. J. Physiol. Pharmacol.* **1995**, *73*, 55. (c) Reul, B. A.; Amin, S. S.; Buchet, J. P.; Ongemba, L. N.; Crans, D. C.; Brichard, S. M. *Br. J. Pharm.* **1999**, *126*, 467. (d) Sakurai, H.; Sano, H.; Takino, T.; Yasui, H. *J. Inorg. Biochem.* **2000**, *80*, 99.

(2) (a) Goldfine, A. B.; Simonson, D. C.; Folli, F.; Patti, M. E.; Kahn, C. R. *J. Clin. Endocrinol. Metab.* **1995**, *80*, 3311. (b) Halberstam, M.; Cohen, N.; Shlimovich, P.; Rossetti, L.; Shamoon, H. *Diabetes* **1996**, *45*, 659. (c) Boden, G.; Chen, X.; Ruiz, J.; van Rossum, G.; Turco, S. *Metabolism* **1996**, *45*, 1130.

(3) (a) Makinen, M. W.; Brady, M. J. *J. Biol. Chem.* **2002**, *277*, 12215. (b) Ou, H.; Yan, L.; Mustafi, D.; Makinen, M. W.; Brady, M. J. Manuscript submitted for publication.

(4) (a) Shechter, Y.; Karlish, S. J. D. *Nature* **1980**, *284*, 556. (b) Shechter, Y.; Shisheva, A.; Lazae, R.; Libman, J.; Shanzer, A. *Biochemistry* **1992**, *31*, 2063. (c) Li, J.; Elberg, G.; Crans, D. C.; Shechter, Y. *Biochemistry* **1996**, *35*, 8314.

(5) Abbreviations: acac, acetylacetonato; ENDOR, electron nuclear double resonance; EPR, electron paramagnetic resonance; hf, hyperfine; hfc, hyperfine coupling; malto, maltolato; rf, radio frequency; shf, superhyperfine; $VO(acac)_2$, bis(acetylacetonato)oxovanadium(IV); $VO(malto)_2$, bis(maltolato)oxovanadium(IV).

10.1021/ic040120y CCC: $30.25
Published on Web 07/06/2005

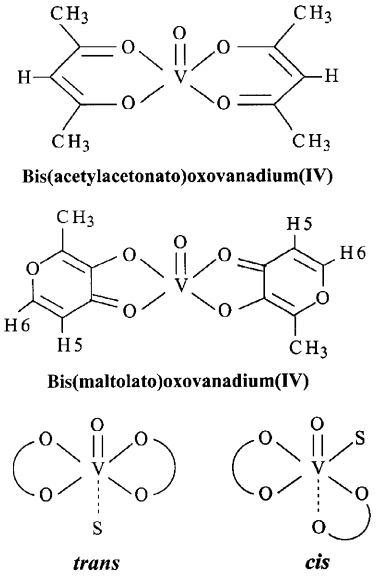

Figure 1. Illustration of chemical bonding structures of bis(acetylacetonato)oxovanadium(IV) and bis(maltolato)oxovanadium(IV). The chelating ligands in both complexes are shown as square-pyramidal complexes in a *trans* conformation, in which the four equatorial coordination sites are occupied by donor ligand atoms of the two chelating ligand molecules. The atomic numbering of the hydrogens in the maltolato ligands reflects standard nomenclature for naming maltol as 3-hydroxy-2-methyl-4-pyrone. In the lowermost part, *trans* and *cis* conformations of the coordinating ligands are schematically illustrated. In this Article, designation of the vanadyl group as V═O is used synonymously with VO^{2+}, as in publications by others. We point out, however, that the electronic bonding structure of the VO^{2+} moiety is analyzed as triple-bonded according to Ballhausen and Gray.[9]

VO^{2+} moiety, stripped of its organic chelating ligands.[6b] These combined observations suggest, therefore, that $VO(acac)_2$ and $VO(malto)_2$ differ structurally with respect to interactions with insulin-signaling molecules.

Figure 1 illustrates the square-pyramidal coordination geometry of $VO(acac)_2$ and $VO(malto)_2$ in crystals in which the chelating ligands are equatorially positioned in a *trans* conformation.[7,8] Although determination of the structure and conformation of organic chelates of VO^{2+} is best achieved through X-ray diffraction of crystals, it is expected that the chelating ligands can adopt *cis* and *trans* conformations in solution. Since the coordination chemistry of VO^{2+} in solution comprises a rich assortment of organic ligands associated with a wide range of binding affinities, structural isomerizations, and pH- or solvent-dependent polymerization reactions,[10] the structure in crystalline form may not correspond to the conformer of highest population in solution. Application of methods such as nuclear magnetic resonance for structural characterization of VO^{2+} chelates is not

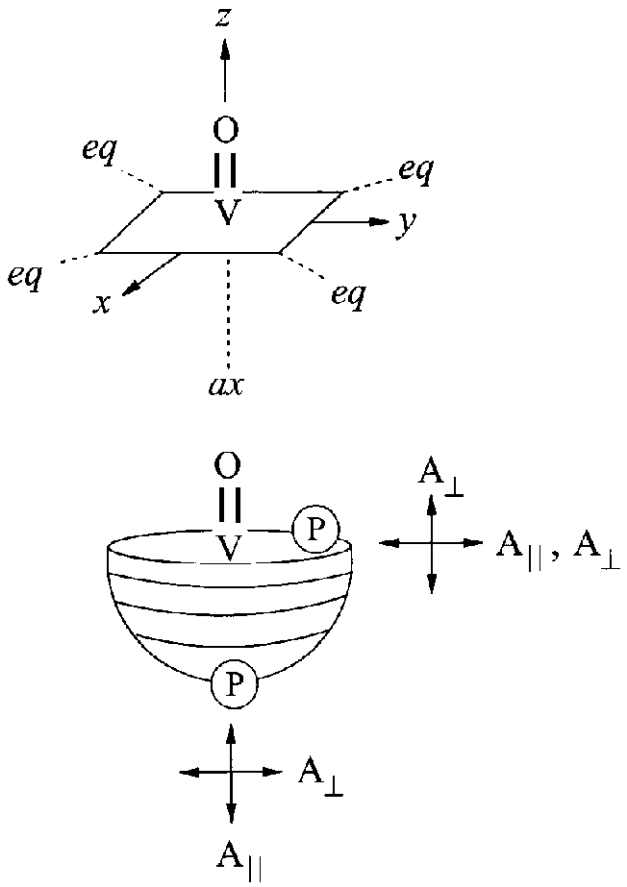

Figure 2. Schematic illustration of the relationships of the symmetry axes of VO^{2+} to the principal axes of the $\mathbf{g}_e$ matrix and of the hf tensor of nearby protons. The top diagram illustrates the direction of the molecular axes with respect to the V═O bond. Four equatorial positions and one axial position are shown that are available for ligand binding. The bottom diagram illustrates the relative positions of protons near the molecular *x*,*y* plane and near or along the *z* axis. Each circle represents an orientation of $\mathbf{H}_0$ within the *g* axis system. This diagram also illustrates the principal hfc components that are detected for equatorially or axially positioned protons according to whether $\mathbf{H}_0$ is coincident with or perpendicular to the *z* axis.

straightforward because of the paramagnetism of the VO^{2+} ion. The unpaired electron is localized in a metal 3d orbital lying along the *x* and *y* axes for the coordinate system shown in the upper part of Figure 2.[11] To overcome this problem, it is necessary to employ a method of structural analysis that takes advantage of the paramagnetism.

The VO^{2+} ion as a spectroscopic probe provides special advantages for structural characterization of coordination complexes in solution by electron magnetic resonance methods. The VO^{2+} ion is one of the most stable diatomic cations known. Its paramagnetism due almost entirely to spin angular momentum is well behaved, and electron paramagnetic resonance (EPR) absorption is observed over a wide

(6) (a) Pandey, S. K.; Anand-Srivastava, M. B.; Srivastava, A. K. *Biochemistry* **1998**, *37*, 7006. (b) Peters, K. G.; Davis, M. G.; Howard, B. W.; Pokross, M.; Rastogi, V.; Diven, C.; Greis, K. D.; Eby-Wilkens, E.; Maier, M.; Evdokimov, A.; Soper, S.; Genbauffe, F. *J. Inorg. Biochem.* **2003**, *96*, 321.
(7) (a) Dodge, R. P.; Templeton, D. H.; Zalkin, A. *J. Chem. Phys.* **1961**, *35*, 55. (b) Amin, S. S.; Cryer, K.; Zhang, B.; Dutta, S. K.; Eaton, S. S.; Anderson, O. P.; Miller, S. M.; Reul, B. A.; Brichard, S. M.; Crans, D. C. *Inorg. Chem.* **2000**, *39*, 406.
(8) Caravan, P.; Gelmini, L.; Glover, N.; Herring, F. G.; Li, H.; McNeil, J. H.; Rettig, S. J.; Setyawati, I. A.; Shuter, E.; Sun, Y.; Tracey, A. S.; Yuen, V. G.; Orvig, C. *J. Am. Chem. Soc.* **1995**, *117*, 12759.
(9) Ballhausen, C. J.; Gray, H. B. *Inorg. Chem.* **1962**, *1*, 111.
(10) (a) Chasteen, N. D. *Struct. Bonding (Berlin)* **1983**, *53*, 105. (b) Chasteen, N. D., Ed. *Vanadium in Biological Systems: Physiology and Biochemistry*; Kluwer Academic Publishers: Boston, 1990; p 225. (c) Sigel, H., Sigel, A., Eds. *Metal Ions in Biological Systems, Vol. 31, Vanadium and Its Role in Life*; Marcel Dekker: New York, 1995; p 779. (d) Tracey, A. S., Crans, D. C., Eds. *Vanadium Compounds: Chemistry, Biochemistry and Therapeutic Applications*; American Chemical Society Symposium Series No. 711, Oxford University Press: New York, 1998; p 381.
(11) (a) Kivelson, D.; Lee, S. K. *J. Chem. Phys.* **1964**, *41*, 1896. (b) Stewart C. P.; Porte, A. L. *J. Chem. Soc., Dalton Trans.* **1972**, 1661.

temperature range, including room temperature. When VO^{2+} is in a site of exact or near square-pyramidal symmetry, the principal directions of its $\mathbf{g}_e$ matrix are readily related to molecular axes with the g_{zz} or $g_{||}$ component coincident with the V=O bond.[11] On this basis, Attanasio showed that the principal values of the hyperfine tensors of nearby protons of Schiff base complexes of VO^{2+} in frozen solution could be determined by electron nuclear double resonance (ENDOR) to extract structural information with high precision.[12a,b] Also, Branca and co-workers have applied this approach to characterize VO^{2+} complexes formed with diphenolic ligands.[12c] We have described a general stratagem for ENDOR-based structural analysis of VO^{2+} complexes in (frozen) solution.[13] Application of this stratagem based on microwave power saturation of the turning points in the EPR spectrum, as first noted by Rist and Hyde,[14] leads directly to collection of ENDOR spectra for which the principal hyperfine coupling components exhibit axial symmetry and are oriented parallel and perpendicular to the V=O bond. Through application of this approach known as angle-selected ENDOR, we have assigned the solvation structure of VO^{2+},[13c] the molecular structure and conformation of nucleotide complexes of VO^{2+},[15] and the coordination environment of VO^{2+} bound to Ca^{2+}-binding proteins.[16] Here we present spectroscopic results defining the molecular structure and conformation of $VO(acac)_2$ and $VO(malto)_2$ in solution.

The X-ray structures of both $VO(acac)_2$[7] and $VO(malto)_2$[8] in crystals show only equatorially positioned organic chelating ligands in a *trans* conformation with no axially coordinated or hydrogen-bonded solvent. In this investigation, we show by application of ENDOR spectroscopy that the structure of the $VO(acac)_2$ complex in solution is not unlike that in crystals[7] except for axially bound solvent coordinated to the metal ion and hydrogen-bonded to the vanadyl oxygen atom. In contrast, while the $VO(malto)_2$ complex exhibits a *trans* conformation in crystals with no metal-coordinated solvent,[8] in solution the organic chelating ligands were found to adopt a *cis* conformation in which the axial position was occupied by a maltolato donor oxygen atom and a solvent molecule was equatorially coordinated. The results of these investigations demonstrate how differently both complexes behave in solution despite chemically similar donor ligand atom environments of the central VO^{2+} moiety. These structural differences likely influence their behavior with insulin-signaling molecules.

Experimental Methods

$VO(acac)_2$ was purchased from Aldrich Chemical Co., Inc. (Milwaukee, WI) and used without further purification. $VO(acac\text{-}d_7)_2$ had been synthesized in earlier studies[15c] according to the procedure described for ^{13}C-enriched acetylacetonates of other metal ions.[17] Crystalline $VO(malto)_2$ was a gift from Dr. K. H. Thompson and Professor C. Orvig of the University of British Columbia. Spectroscopic grade methanol and deuterated compounds CD_3OD (99.5%), CD_3OH (99%), and CH_3OD (99%) were obtained from Aldrich.

EPR and ENDOR spectra were recorded by using an X-band Bruker ESP 300E spectrometer, equipped with an Oxford Instruments ESR910 liquid helium cryostat, a Bruker digital ENDOR accessory and ESP 3220 data system for spectrometer control, data acquisition and processing, and communications, as previously described.[15b,16b] Typical experimental conditions for EPR were sample temperature 20 K, microwave frequency 9.46 GHz, incident microwave power 64 μW (full power 640 mW at 0 dB), modulation frequency 12.5 kHz, and modulation amplitude 0.5 G. Typical experimental conditions for ENDOR were microwave power 6.4 mW, rf power 50 W, rf modulation frequency 12.5 kHz, and rf modulation depth 8−10 kHz. The static laboratory magnetic field was not modulated for ENDOR. The concentration of VO^{2+} compounds in methanol for EPR and ENDOR studies was 5.0×10^{-3} M. The solvent was purged with nitrogen gas before use, and samples were stored in liquid nitrogen.

Molecular modeling was carried out with use of Insight97 (Accelrys, San Diego, CA) running on an SGI R4400 Indigo^2 workstation with Solid Impact graphics. Atomic coordinates of non-hydrogen atoms of $VO(acac)_2$ and $VO(malto)_2$ were taken from X-ray crystallographic studies.[7,8] Atomic coordinates of hydrogen atoms were calculated according to idealized bond lengths and valence angles.[18]

Results and Discussion

A. Characteristics of ENDOR Spectra at Selected Molecular Orientations. ENDOR spectroscopy is carried out by "pumping" the electron-spin-allowed transitions of the paramagnetic system under high microwave power and irradiating simultaneously with a strong rf field. When the frequency of the rf field is scanned under these conditions and resonance of a nucleus interacting with the unpaired electron is reached, a forbidden transition equivalent to simultaneous electron and nuclear "spin flips" is stimulated, giving rise to increased EPR signal amplitude. Thus, the ENDOR method has its basis in detection of nuclear resonance absorption by observing changes in the intensity of EPR absorption.

We have discussed the physical and theoretical basis of angle-selected ENDOR applied to the VO^{2+} ion.[13] Here we summarize only those aspects that are particularly pertinent to structural analysis with use of VO^{2+} as the paramagnetic probe. For VO^{2+} complexes, the g_{zz} or $g_{||}$ component of the $\mathbf{g}_e$ matrix is critical for selection of molecular orientation.

(12) (a) Attanasio, D. *J. Phys. Chem.* **1986**, *90*, 4952. (b) Attanasio, D. *J. Chem. Soc., Faraday Trans. 1* **1989**, *85*, 3927. (c) Branca, M.; Micera, G.; Dessi, A. *J. Chem. Soc., Dalton Trans.* **1990**, 457.

(13) (a) Makinen, M. W.; Mustafi D. In *Metal Ions in Biological Systems*; Sigel, H., Sigel, A., Eds.; Marcel Dekker: New York, 1995; Vol. 31, pp 89−127. (b) Mustafi, D.; Makinen, M. W. In *Biological Magnetic Resonance*; Eaton, G. A., Eaton, S., Berliner, L. J., Eds.; Plenum Press: New York, 2004; Vol. 24, pp 89−144. (c) Mustafi, D.; Makinen, M. W. *Inorg. Chem.* **1988**, *27*, 3360.

(14) (a) Rist, G. H.; Hyde, J. S. *J. Chem. Phys.* **1968**, *49*, 2449. (b) Rist, G. H.; Hyde, J. S. *J. Chem. Phys.* **1970**, *52*, 4633.

(15) (a) Mustafi, D.; Telser, J.; Makinen, M. W. *J. Am. Chem. Soc.* **1992**, *114*, 6219. (b) Jiang F. S.; Makinen, M. W. *Inorg. Chem.* **1995**, *34*, 1736. (c) Mustafi, D.; Bekesi, A.; Vertessy, B. G.; Makinen, M. W. *Proc. Natl. Acad. Sci. U.S.A.* **2003**, *100*, 5670.

(16) (a) Mustafi, D.; Nakagawa, Y. *Biochemistry* **1996**, *35*, 14703. (b) Mustafi, D.; Nakagawa, Y. *Proc. Natl. Acad. Sci. U.S.A.* **1994**, *91*, 11323. (c) Mustafi, D.; Nakagawa, Y.; Makinen, M. W. *Cell. Mol. Biol.* **2000**, *46*, 1345. (d) Lee, B. I.; Mustafi, D.; Cho, W.; Nakagawa, Y. *J. Biol. Inorg. Chem.* **2003**, *8*, 341.

(17) Junge, H.; Musso, H.; Zahorszky, UI. *Chem. Ber.* **1968**, *101*, 793.

(18) Coppens, P. *Science* **1967**, *158*, 1577.

Setting $\mathbf{H}_0$ to the $-7/2$ parallel component of the EPR spectrum selects those molecules for which the V═O bond or $g_{\|}$ component of the $\mathbf{g}_e$ matrix is parallel to the laboratory magnetic field, i.e., the equatorial *x*,*y* plane is perpendicular to $\mathbf{H}_0$. Correspondingly, setting $\mathbf{H}_0$ to the $-3/2$ perpendicular component of the EPR spectrum of VO^{2+} selects molecules for which the laboratory field is contained within the *x*,*y* molecular plane, i.e., $\mathbf{H}_0$ is perpendicular to the V═O bond.

Figure 2 illustrates the expected pattern of observed ENDOR splittings as a function of the positions of protons and the orientation of $\mathbf{H}_0$ with respect to $g_{\|}$ of VO^{2+}. When $\mathbf{H}_0$ is within a small conical sector of being perpendicular to the molecular plane, i.e., parallel to the V═O bond, a parallel hyperfine coupling $A_{\|}$ of a proton located along the symmetry axis is observed, labeled "ax" for axial protons, or a perpendicular hyperfine coupling component $A_{\perp}$ of a proton located near or in the *x*,*y* plane is observed, labeled "eq" for equatorial protons.[19] On the other hand, if $\mathbf{H}_0$ is perpendicular to the V═O bond, i.e., in the molecular *x*,*y* plane, $A_{\perp}$ of an axial proton and both $A_{\|}$ and $A_{\perp}$ of an equatorial proton are observed.

When *g* anisotropy is small compared to the average *g* value, as in the case of VO^{2+}, the maximum hf interaction energy occurs for a field oriented along the electron−nucleus vector (A_z axis), and the minimum occurs when the field is in the A_x,A_y plane. For a proton in the *x*,*y* plane, well-resolved features corresponding to $A_{\perp}$ are observed which persist with an essentially constant ENDOR shift at all $\mathbf{H}_0$ values.[20] This observation is an important diagnostic characteristic, particularly under conditions of low signal-to-noise ratio, since $A_{\|}$ couplings reach a maximum splitting dependent on $\mathbf{H}_0$. Thus, variation in the magnitude of the splitting with a change in the $\mathbf{H}_0$ setting serves as the experimentally derived criterion to assign hf couplings to parallel or perpendicular components. For an equatorially located proton, both $A_{\|}$ and $A_{\perp}$ are observed when the magnetic field orientation $\mathbf{H}_0$ is near or in the molecular *x*,*y* plane. These relationships provide the basis to analyze hf interactions in terms of nuclear coordinates. For VO^{2+} complexes, we have observed hitherto only axially symmetric hf interactions such that each structural class of protons gives rise to only $A_{\|}$ and $A_{\perp}$ couplings.

B. ENDOR of $VO(acac)_2$. 1. Assignments of Proton ENDOR Absorptions. For a system of low *g* anisotropy, as in the case of VO^{2+}, the first-order ENDOR transition frequencies $\nu_{\pm}$ within the strong-field approximation are given by eq 1. The separation of $\nu_{\pm}$ about the nuclear Larmor

$$\nu_{\pm} = \nu_n \pm |A|/2 \qquad (1)$$

frequency ν_n is called the ENDOR shift. For symmetric separations, the hf coupling is, thus, equal to twice the value of this frequency shift. Equation 1 applies to the condition $\nu_n > |A|/2$, which is characteristic of ^{1}H discussed here. For some nuclei, e.g., ^{2}H, the condition $\nu_n < |A|/2$ may apply, in which case eq 1 becomes $\nu_{\pm} = |A|/2 \pm \nu_n$.

For $VO(acac)_2$, identification of the structural origins of resonance features has rested on site-specific incorporation of deuterium into the organic ligand. While the resonance assignments of the methyl groups are readily confirmed because of their high intensity, identification of resonances of the bridging hydrogens has been problematic because of their low intensity and because of their tendency to undergo proton exchange with solvent.[21] Since the last step in the synthesis of $VO(acac)_2$ requires crystallization of the complex from acidic media, it is necessary to employ D_2O for crystallization to ensure high levels of deuterium enrichment in the synthesis of perdeuterated $VO(acac)_2$. Thus, through use of differentially deuterated forms of methanol and the perdeuterated VO^{2+} chelate, we have been able to assign the weak resonance features of the bridging hydrogens and to separate them from resonance features belonging to the methyl and hydroxyl hydrogens of the solvent methanol. Furthermore, by taking advantage of the tendency of the bridging hydrogens to undergo proton or deuteron exchange, assignments of the resonances of the bridging hydrogens could be confirmed independent of the isotope composition of the methyl groups. In earlier ENDOR studies of $VO(acac)_2$ by others,[22,23] manipulation of the isotope composition of the organic ligand was not attempted for spectroscopic assignments.

Figure 3 illustrates the proton ENDOR spectra of $VO(acac)_2$ in methanol of natural abundance isotope composition and in deuterated methanol with the $\mathbf{H}_0$ setting at the $-3/2$ perpendicular EPR feature. The topmost spectrum shows all proton resonance features from $VO(acac)_2$ and methyl and hydroxyl protons of solvent methanol molecules. Comparison of this spectrum with spectra II and III for $VO(acac)_2$ dissolved in CD_3OH and CD_3OD, respectively, identifies the parallel and perpendicular hfc components of the bridging (H^{CH}) and methyl (H^{CH_3}) protons of the acetylacetonato ligand, indicated with solid-line stick diagrams. The resonance features for the hydroxyl and methyl protons of solvent methanol molecules, identified similarly on the basis of differentially deuterated forms of the solvent, are indicated with dotted-line stick diagrams and are labeled A−G. In spectrum III the intensity of resonance features for H^{CH} is reduced from that in spectrum II. Also, in spectrum III a broad ENDOR feature of very low amplitude is observed with an approximate 3.0 MHz splitting, corresponding to that of the prominent resonance labeled A. This feature is typically observed for an axially coordinated hydroxyl group.[13−15] Since this broad resonance feature is retained in spectrum IV for VO(acac-d_7)$_2$ in CD_3OD without

(19) The mathematical relationships underlying these observations apply for all angles of the conical sector $0° \le \phi < 90°$. However, the peak-to-peak amplitude of the observed resonance feature becomes the limiting constraint. In general, we have observed resonance features only when $\mathbf{H}_0$ lies within ±15° of being coincident with the symmetry axis or perpendicular to the axis.

(20) (a) Hurst, G. C.; Henderson, T. A.; Kreilick, R. W. *J. Am. Chem. Soc*. **1985**, *107*, 7294. (b) Henderson, T. A.; Hurst, G. C.; Kreilick, R. W. *J. Am. Chem. Soc.* **1985**, *107*, 7299.
(21) Angerman, N. S.; Jordan, R. B. *Inorg. Chem.* **1969**, *8*, 1824.
(22) (a) van Willigen, H. *Chem. Phys. Lett.* **1979**, *65*, 490. (b) Kirste, B.; van Willigen, H. *J. Phys. Chem.* **1982**, *86*, 2743.
(23) Yordanov, N. D.; Zdravkova, M. *Polyhedron* **1993**, *12*, 635.

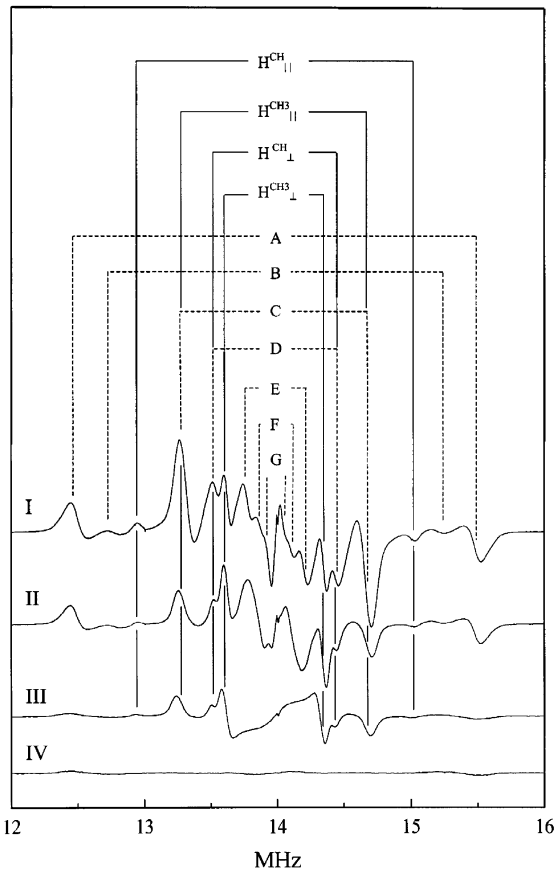

Figure 3. Proton ENDOR spectra of $VO(acac)_2$ as a function of deuteration with $\mathbf{H}_0$ set to the −3/2 perpendicular EPR spectral component. The spectra are indicated as follows: I, $VO(acac)_2$ in CH_3OH; II, $VO(acac)_2$ in CD_3OH; III, $VO(acac)_2$ in CD_3OD; IV, VO(acac-d_7) in CD_3OD. The ENDOR absorption features are identified in the stick diagram and are equally spaced about the proton Larmor frequency of 13.99 MHz. The solid lines are drawn for the parallel and perpendicular hfc components of the bridging −CH− proton ($H^{CH}_{||}$ and $H^{CH}_{\perp}$) and methyl protons ($H^{CH_3}_{||}$ and $H^{CH_3}_{\perp}$) of $VO(acac)_2$, while the dashed lines (A−G) are drawn for solvent protons.

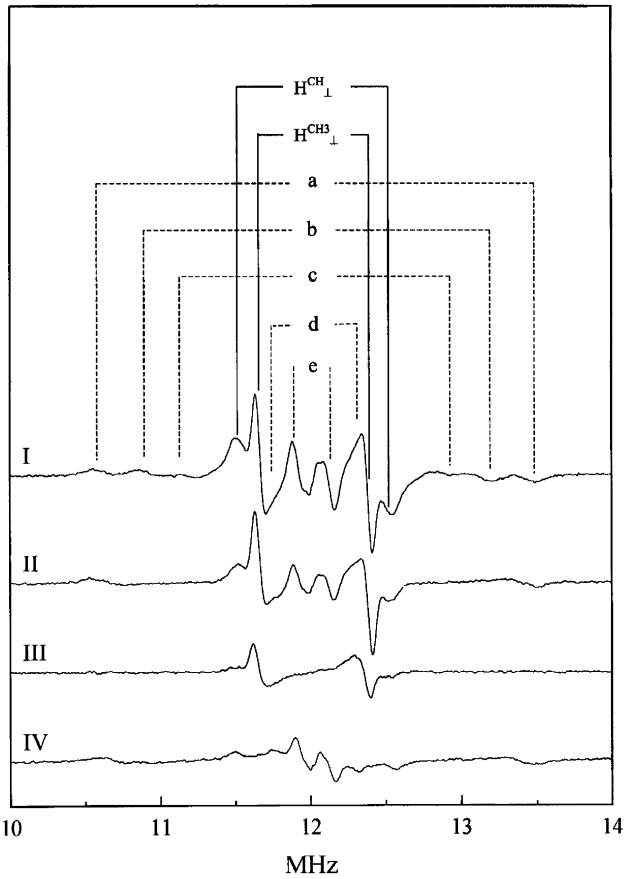

Figure 4. Proton ENDOR spectra of $VO(acac)_2$ as a function of deuteration with $\mathbf{H}_0$ set to the −7/2 parallel EPR spectral component. The spectra are labeled as in Figure 3: I, $VO(acac)_2$ in CH_3OH; II, $VO(acac)_2$ in CD_3OH; III, $VO(acac)_2$ in CD_3OD; IV, VO(acac-d_7) in CD_3OH. The ENDOR absorption features are identified in the stick diagram and are equally spaced about the free proton frequency of 11.90 MHz. The solid lines are drawn for the perpendicular hfc components of the bridging −CH− proton ($H^{CH}_{\perp}$) and methyl protons ($H^{CH_3}_{\perp}$) of $VO(acac)_2$, while the dashed lines (a−e) are drawn for solvent protons.

a change in intensity, we conclude that it must come from the residual hydroxyl proton content of CD_3OD.

Figure 4 similarly illustrates the proton ENDOR spectra of $VO(acac)_2$ as in Figure 3 but with the $\mathbf{H}_0$ setting at the −7/2 parallel EPR feature. At this magnetic field setting, a "single-crystal-type" ENDOR spectrum should be observed.[14] According to Figure 2, only the perpendicular hfc components will be observed for a coordination complex in which all organic hydrogens are located in the equatorial plane. There is a similar loss of intensity between spectra II and III showing a decrease in resonance absorption overlapping with that of H^{CH}, as described for Figure 3 and assigned to the residual hydroxyl proton content of CD_3OD. The bottommost spectrum of VO(acac-d_7)$_2$ in CD_3OH shows the perpendicular hfc component of H^{CH} along with residual hydroxyl protons of the solvent. The structural origins and principal values of the hfc components for all resonance features of $VO(acac)_2$ are summarized in Table 1. Values of ENDOR-based electron−nucleus distances estimated on the basis of eq 2, described below, are also included. Since individual methyl protons were not resolved in ENDOR spectra, the calculated electron−nucleus distance is applied to the geometrically averaged methyl proton.

Table 1. Summary of hfc Components[a] and Estimated Vanadium−Proton Distances in Bis(acetylacetonato)oxovanadium(IV) in Frozen Methanol

$A_{||}$	$A_{\perp}$	A_{iso}	$A_{||}^{D}$	$A_{\perp}^{D}$	r (Å)	comment
			acac			
2.02	0.91	0.07	1.95	−0.98	4.28 ± 0.10	H^{CH}
1.47	0.75	0.01	1.48	−0.74	4.70 ± 0.10	H^{CH_3}
			Solvent			
6.00	3.01	0.01	6.01	−3.00	2.94 ± 0.06	OH axial
2.35	1.40	−0.15	2.50	−1.25	3.93 ± 0.10	CH_3 axial
4.46[b]	1.00	0.55	3.91	−1.95	3.40 ± 0.12	OH, H-bonded[c]
0.82	0.44	−0.02	0.84	−0.42	5.66 ± 0.31	CH_3, H-bonded[c]
2.67	0.51	0.55	2.12	−1.06	4.16 ± 0.23	OH, outer-sphere[d]
1.83	0.20	0.48	1.35	−0.68	4.84 ± 0.28	CH_3, outer-sphere[d]

[a] hfc components are in units of megahertz. Uncertainty in the ENDOR shift of 20−30 kHz estimated from the line width of ENDOR absorption is included as the uncertainty in the calculation of electron−proton distances in accord with previous studies.[13,15,16] [b] A very broad peak was observed. [c] This corresponds to an axially located methanol molecule which is hydrogen-bonded to the vanadyl oxygen atom ($V{=}O{\cdots}HOCH_3$).[13c] [d] This corresponds to an axially located, outer-sphere methanol molecule. No ENDOR feature was observed that could be assigned to an equatorially located, outer-sphere methanol molecule.

2. Analysis of ENDOR Splittings and Estimation of Metal−Proton Distances in $VO(acac)_2$. Within the strong-field approximation, the observed hf coupling A is given by

eq 2 as a function of r and α where h is the Planck constant,

$$A = \frac{g_N|\beta_N|g_e|\beta_e|}{hr^3}(3\cos^2\alpha - 1) + A_{iso} \qquad (2)$$

r is the modulus of the electron−nucleus position vector **r**, and α is the angle between $\mathbf{H}_0$ and **r**. For VO^{2+} complexes, the observed principal hfc components $A_{||}$ and $A_{\perp}$ correspond, respectively, to the maximum and minimum ENDOR shifts. The principal hfc components due to dipole−dipole interaction, $A_{||}^D$ and $A_{\perp}^D$, correspond to the first term of eq 2 for values of $\alpha = 0°$ and 90°, respectively. Under the conditions $|A_{iso}| \ll |A_{||}|$ and $|A_{\perp}|$, and $A_{||}^D > 0 > A_{\perp}^D$, the traceless dipolar hfc components $A_{||}^D$ and $A_{\perp}^D$ can be calculated under the constraint $A_{||} + 2A_{\perp} = 3A_{iso}$. In Table 1 we have summarized our estimates of the principal hfc components and isotropic couplings for each class of protons, along with the calculated metal−proton separations. The latter are based on application of the stratagem outlined above and described in earlier studies.[13,15,16]

The pseudocontact contribution to the isotropic hf coupling, represented as the second right-hand term in eq 2, is negligible in cases of low g anisotropy. We have, therefore, made the approximation that A_{iso} arises entirely from the Fermi contact term. Because the unpaired electron is localized to a metal 3d orbital in VO^{2+} with lobes directed along the x and y axes in the coordinate axis system in Figure 2, the transfer of unpaired spin density to equatorially positioned ligand atoms is small.[11,13] Snetsinger et al. have shown that attributing the observed hf coupling of an unpaired electron in such a metal 3d orbital entirely to the dipole−dipole interaction with a nuclear spin of $I = 1/2$ over a distance of 2.09 Å results in a calculated separation of 2.15 Å.[24] Since the contribution of the isotropic hfc is less for larger electron−nucleus distances, the error will be correspondingly smaller.

In earlier ENDOR studies of $VO(acac)_2$ in frozen methanol, a resonance feature with an hf coupling of ∼3.4 MHz was assigned to H^{CH} of the acetylacetonato ligand.[22] For $VO(acac)_2$ in frozen chloroform, Yordanov and Zdravkova[23] assigned a resonance feature with a similar ENDOR shift to a solvent molecule hydrogen-bonded to the equatorial oxygen donor atoms. We note that high rf amplitude modulation (∼50−80 kHz) was applied in these studies.[22,23] We have been unable to detect these features under the much reduced rf amplitude modulation conditions (≤10 kHz) employed in our experiments. As listed in Table 1, the value of A_{iso} for H^{CH} is very small (∼0.07 MHz), and the assignment was confirmed on the basis of selectively deuterated materials. As shown below, our estimate of the vanadium−proton distance of 4.28 ± 0.10 Å for H^{CH} is in excellent agreement with X-ray-defined coordinates.

C. ENDOR of $VO(malto)_2$: Assignments of ENDOR Features and Estimation of Metal−Proton Distances. The assignments of proton ENDOR features in $VO(malto)_2$ were made similarly to those for $VO(acac)_2$. Although we did not have access to a selectively deuterated complex, as in the case of $VO(acac)_2$, we have been able to make, nonetheless, critical resonance assignments for defining the conformation of the organic ligands with respect to the magnetic axes of the VO^{2+} moiety.

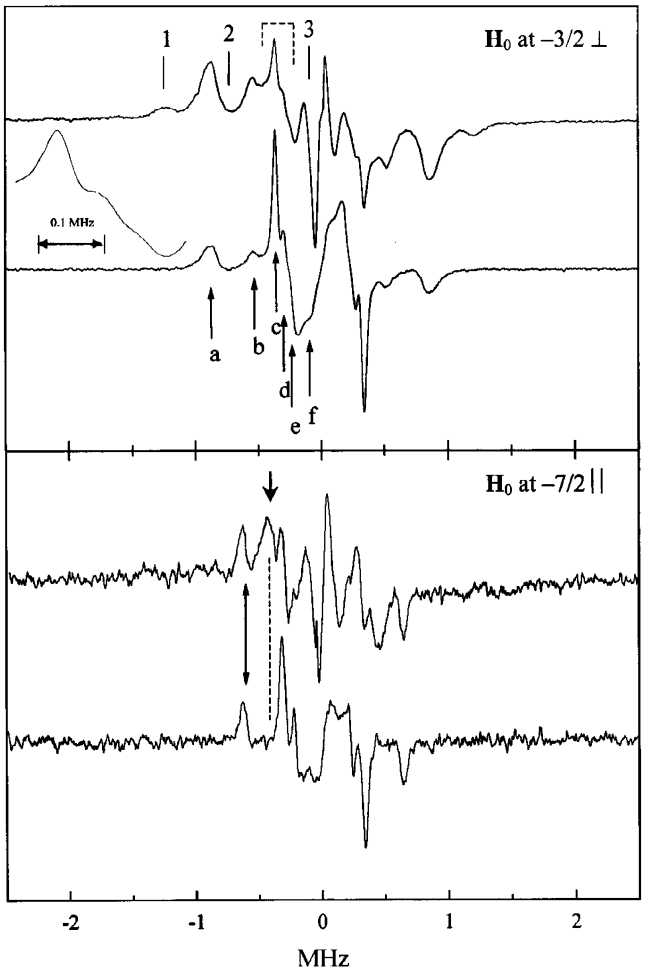

Figure 5. Proton ENDOR spectra of $VO(malto)_2$ in methanol. In the upper panel, the laboratory magnetic field $\mathbf{H}_0$ was set to the −3/2 perpendicular EPR spectral component; in the lower panel, $\mathbf{H}_0$ was set to the −7/2 parallel EPR spectral component. In each panel, the upper spectrum represents the compound dissolved in CH_3OH while the lower spectrum represents the compound in CD_3OD. The abscissa measures the observed ENDOR shift, $\Delta\nu = \nu_{ENDOR} - \nu_H$, where ν_{ENDOR} represents the observed frequency and ν_H represents the proton Larmor frequency. In the upper panel, three ENDOR features, labeled 1−3, are assigned to protons from solvent molecules while six ENDOR features indicated by arrows a−f are assigned to protons from the maltolato ligands. In the upper panel, the area indicated by dashed lines at the top of the diagram is shown with an expanded scale to the left. Three hfc components labeled c−e are resolved. In the lower panel, two new features not present in the upper panel are indicated by arrows. The ENDOR feature indicated by a down arrow is observed only in the upper spectrum, the dashed line indicating that this feature is absent in the lower spectrum for $VO(malto)_2$ in CD_3OD. The feature indicated by a double-headed arrow is observed in both spectra and, therefore, has its origin in the maltolato ligand. Three remaining line pairs (c, e, and f) in the lower spectrum of the lower panel are identical to those in the lower spectrum of the upper panel. They are not labeled. All line splittings in this figure and their assignments are listed in Table 2.

Figure 5 illustrates the proton ENDOR spectra of $VO(malto)_2$ in methanol with $\mathbf{H}_0$ settings at both the −3/2 perpendicular and −7/2 parallel EPR features. Each panel compares the spectrum of $VO(malto)_2$ in methanol of natural abundance isotope composition to the spectrum of

(24) Snetsinger, P. A.; Chasteen, N. D.; van Willigen, H. *J. Am. Chem. Soc.* **1990**, *112*, 8155.

Table 2. Observed Proton ENDOR Splittings (in MHz) of Bis(maltolato)Oxovanadium(IV) in Frozen Methanol

$\mathbf{H}_0$ setting	line pair[a]	line splitting	assignment
−3/2 perpendicular	1	2.44	∥ OH proton, equatorial outer-sphere
	2	1.48	⊥ OH proton, axial V═O···H
	3	0.28	⊥ OH proton, equatorial outer-sphere
	a	1.73	∥ maltolato, equatorial
	b	1.07	∥ maltolato, equatorial
	c	0.67	⊥ maltolato, equatorial
	d	0.62	∥ maltolato, equatorial
	e	0.47	⊥ maltolato, equatorial
	f	0.23	⊥ maltolato, equatorial
−7/2 parallel	double-headed arrow	1.29[b]	∥ maltolato, axial
	down arrow	0.84[b]	⊥ OH proton, equatorial inner-sphere
	c	0.67	⊥ maltolato, equatorial
	e	0.47	⊥ maltolato, equatorial
	f	0.23	⊥ maltolato, equatorial

[a] Line pairs are assigned in Figure 5. [b] These two ENDOR features are observed only with $\mathbf{H}_0$ at −7/2 parallel EPR absorption.

$VO(malto)_2$ in perdeuterated methanol. On this basis, the upper spectrum in each panel contains all resonance features from $VO(malto)_2$ and methanol as the solvent while the lower spectrum in each panel illustrates proton resonance features only from the $VO(malto)_2$ complex. The three resonance features labeled 1−3 in the upper panel are assigned to solvent because they are absent for the compound dissolved in CD_3OD. On the other hand, in the upper panel, six pairs of resonance features, the lower frequency components of which are labeled with arrows a−f, have their origin in the chelating ligand. As seen in Figure 1, there are three classes of protons in $VO(malto)_2$ labeled H5, H6, and CH_3. We assign the six resonance features to the parallel and perpendicular hfc components of these three classes of protons in this VO^{2+} complex. Three of these resonance features c, e, and f, appear in the −7/2 parallel spectrum in the lower panel with identical splittings, indicating that they correspond to perpendicular hf couplings. Since protons in the organic ligand can be expected to have near-negligible values for A_{iso} because of their distance from the VO^{2+} ion, as observed in Table 1 for $VO(acac)_2$, the magnitudes of the counterpart parallel hf couplings of resonance features c, e, and f should track with the magnitudes of the perpendicular hf couplings; also, for equatorial ligands, they should appear in the spectrum with $\mathbf{H}_0$ set to the −3/2 perpendicular EPR spectral component. On this basis, we paired resonance features a, b, and d with c, e, and f, respectively. In this manner, we found that the estimates of the electron−proton distances for the three classes of covalent hydrogens associated with the maltolato ligand corresponded closely to vanadium−proton separations calculated on the basis of the X-ray description[8] of the $VO(malto)_2$ complex.

In the lower panel of Figure 5, two additional features are seen. One identified by the "down" arrow must belong to solvent since it is absent in the bottom spectrum for the compound dissolved in perdeuterated methanol. The other feature identified by a double-headed arrow is very sharp and must arise from a covalent hydrogen in the maltolato ligand because it is seen in both spectra in the lower panel. To assign the origin of this resonance absorption, we refer to Figure 2. Since this resonance feature is detected only in the −7/2 parallel spectrum, it must arise from a covalently attached hydrogen positioned along the symmetry axis.

Table 3. Summary of hfc Components[a] and Estimated Electron−Proton Distances of *Bis*(maltolato)Oxovanadium(IV) in Frozen Methanol

$A_{\parallel}$	$A_{\perp}$	A_{iso}	$A_{\parallel}^{D}$	$A_{\perp}^{D}$	r (Å)	comment
			Maltolato			
1.73	0.67	0.13	1.60	−0.80	4.57 ± 0.20	H5 (eq)
0.62	0.23	0.05	0.57	−0.28	6.44 ± 0.38	H6 (eq)
1.07	0.47	0.04	1.03	−0.51	5.29 ± 0.28	H^{CH_3} (eq)
1.29			1.29		4.91 ± 0.25	H5 (ax)[b]
			Solvent			
4.46[c]	1.48	0.50	3.96	−1.98	3.39 ± 0.18	OH, H-bonded[d]
2.44	0.28	0.63	1.81	−0.91	4.39 ± 0.23	OH, outer-sphere[e]
	0.84					OH, inner-sphere[f]

[a] hfc components are in units of megahertz. Uncertainty in the ENDOR shift of 20−30 kHz estimated from the line width of ENDOR absorption is included as the uncertainty in the calculation of electron−proton distances. [b] This ENDOR feature was assigned to a parallel hfc component of the maltolato ligand. Since this component appeared only with $\mathbf{H}_0$ at the −7/2 parallel EPR feature, this feature must come from a proton that is located along or near the symmetry axis, i.e., parallel to the V═O bond; see the text. [c] A very broad peak was observed. [d] This is an axially located methanol molecule that is hydrogen-bonded to the vanadyl oxygen atom. [e] This is an equatorially located, outer-sphere methanol molecule. [f] This feature is assigned to an inner-sphere, equatorially located OH proton; see the text.

According to the stratagem described in Figure 2, this resonance feature cannot be assigned to a perpendicular hfc component of an axially located proton because, together with its parallel component, it would have been observed with an approximate ∼2.6 MHz splitting in both −3/2 perpendicular spectra in the upper panel. Since there is no indication of such a resonance feature, we conclude that this sharp ENDOR feature constitutes a parallel hf coupling.

In Table 2 we have listed the chemical origins of each ENDOR splitting detected for $VO(malto)_2$ in methanol. The hfc component for each resonance feature has been assigned on the basis of its appearance in either the −3/2 perpendicular or the −7/2 parallel spectrum, according to Figure 2. As noted above, pairing resonance features a, b, and d with c, e, and f, respectively, in Table 3 yielded estimates of their respective electron−proton distances in close agreement with X-ray estimates for H5, H6, and CH_3. The 0.84 MHz splitting appearing in only the −7/2 parallel spectrum and arising from solvent is identical to the perpendicular hfc component of an equatorially coordinated, inner-sphere solvent hydroxyl group in $[VO(CH_3OH)_4H_2O)]^{2+}$ or $[VO(CH_3OH)_5]^{2+}$ (ref 13c). This resonance feature was, therefore, assigned to the hydroxyl group of an equatorially coordinated methanol

molecule. Comparison of the EPR line width of the −3/2 perpendicular component of $VO(malto)_2$ in ordinary methanol to that in perdeuterated methanol showed a decrease in line width of 1.25 ± 0.10 G, while a corresponding decrease of 0.22 ± 0.10 G was observed for $VO(acac)_2$ (data not shown). According to the analysis of Albanese and Chasteen,[25] the superhyperfine broadening of EPR spectral components of VO^{2+} complexes is observed only for equatorially coordinated ligands. The decrease of 1.25 ± 0.10 G in line width upon introduction of perdeuterated solvent, compatible with only one equatorially coordinated hydroxyl group, thus confirmed the ENDOR assignment of an equatorially coordinated methanol molecule.[26]

From the ENDOR splittings in Table 2, we have made estimates of the principal hfc components and isotropic couplings for each class of protons in the $VO(malto)_2$ complex in methanol.[27] Together with the corresponding ENDOR-based vanadium−proton distances, we have summarized these results in Table 3 to provide a basis for constructing the structure of the $VO(malto)_2$ complex in solution.

D. Molecular Structure and Conformation of $VO(acac)_2$ and $VO(malto)_2$ in Solution Derived on the Basis of ENDOR Distance Constraints. The ENDOR spectra of $VO(acac)_2$ illustrated in Figures 3 and 4 require that the covalent hydrogens of the CH_3- and bridging −CH− groups of both acetylacetonato ligands are positioned in the molecular *x*,*y* plane with respect to the central VO^{2+} moiety, comparable to the X-ray-defined complex.[7] The ENDOR-defined estimates of 4.28 ± 0.10 and 4.70 ± 0.10 Å for the vanadium−H^{CH} and vanadium−H^{CH3} distances, respectively, find complete overlap with the corresponding values of 4.37 and 4.65 Å measured from the X-ray-defined complex. However, comparison of the X-ray-defined $VO(acac)_2$ complex with ENDOR results by modeling requires shortening of V−O bond lengths by ≤0.06 Å and subtle adjustments of O═V−O valence angles by ≤3.0° to achieve overlap of the two structures within the line width-based uncertainties associated with the vanadium−proton distances. These small differences in bond lengths and valence angles reflect the circumstance that a rigid-body approach has been applied in modeling. X-ray diffraction data, averaged over all unit cells in the crystal and over time, do not reflect the dynamic interconversion of the two metal-bound oxygens in each acetylacetonato ligand between keto and ionized hydroxyl states, together with the small alterations in C−C and C═C bond lengths that occur through resonance. Instead, the X-ray-defined complex is a symmetrized molecule in which V−O bond lengths and O═V−O valence angles are virtually indistinguishable from each other.[7] Nonetheless, given the average bond distance and valence angle data for the acetylacetonato ligand and applying a rigid-body fit of the organic ligand to the $VO(O)_4$ fragment according to the electron−nucleus distances in Table 1 resulted in values of 98.3° and 100.9° for the O═V···H^{CH} and O═V···H^{CH_3} angles compared to values of 104.0° and 106.2° in the X-ray structure. This difference indicates only a slight change in the tilt of a planar acetylacetonato ligand with respect to the V═O axis. Since this represents the largest deviation from the X-ray-defined complex with respect to the stereochemistry of the organic ligands, it is evident that the ENDOR results are of high precision.

The primary difference between the X-ray structure of $VO(acac)_2$ and that determined by ENDOR concerns inner- and outer-sphere-coordinated solvent molecules. In the X-ray structure the fifth coordination site opposite the vanadyl oxygen atom is not occupied and the V^{4+} moiety is pentacoordinate with tetragonal-pyramidal geometry. For the complex in solution, the ENDOR spectra yielded unambiguous evidence for an axial, inner-sphere-coordinated methanol. The ENDOR-defined vanadium−H^{OH} and vanadium−H^{CH_3} distances of 2.94 and 3.93 Å, respectively, yielded a linear O═V···O configuration with an axial V−O distance of 2.42 Å, in good agreement with expectation. Close examination of the bond distance and O═V−O valence angle parameters of the equatorial oxygen atoms in the X-ray-defined complex[7] showed them to be fully sterically compatible with an axially coordinated solvent molecule, as in solution. We conclude that the lack of an axial ligand in crystals must be a consequence of molecular packing relationships.

In addition to the axial, metal-coordinated methanol molecule, the ENDOR spectra provided evidence for a methanol molecule hydrogen-bonded to the vanadyl oxygen, as in the solvated structures of $[VO(CH_3OH)_4(H_2O)]^{2+}$ and $[VO(CH_3OH)_5]^{2+}$ (ref 13c). For the methanol molecule hydrogen-bonded to the vanadyl oxygen, the ENDOR-defined vanadium−H^{OH} distance of 3.40 ± 0.12 Å yields a D−H···A separation of 2.79 Å. This value corresponds to the minimum potential energy and most stable configuration for N−H···O or O−H···O hydrogen-bonding interactions.[28] The ENDOR spectra also provided evidence for an axially positioned, outer-sphere methanol molecule (cf. Table 1). As in our earlier ENDOR study of the solvation structure of VO^{2+} (ref 13c), we suggest that outer-sphere solvent molecules were detected because they are likely stabilized through hydrogen-bonding. In this instance, the ENDOR data provided no indication of the location of the outer-sphere methanol with respect to the vanadyl oxygen. Through examination of potential hydrogen-bonding interactions with the axial solvent molecules, outer-sphere-coordinated solvent is likely stabilized as a circular array of structured solvent molecules on both surfaces of the planar acetylacetonato ligands. The ENDOR-assigned structure of $VO(acac)_2$ in

(25) Albanese, N. F.; Chasteen, N. D. *J. Phys. Chem.* **1978**, *82*, 910.

(26) We ascribe the change in line width of 0.22 ± 0.10 G observed for $VO(acac)_2$ under comparable conditions to contributions from H^{CH} in addition to outer-sphere solvent molecules. We have observed a decrease in line width of ≤0.09 G for bis(1-*N*-oxide-2-thiolatopyridine)-oxovanadium(IV)[1c] with no exchangeable hydrogens in the organic chelating ligands (Mustafi, D.; Makinen, M. W. Unpublished observations).

(27) We have observed that ENDOR spectra of $VO(malto)_2$ in aqueous methanol do not differ substantially from those described here for the complex in neat methanol.

(28) Jeffrey, G. A.; Saenger, W. Metrical Aspects of Two-Center Hydrogen Bonds. *Hydrogen Bonding in Biological Structures*; Springer-Verlag: Berlin, 1991; Chapter 7, pp 111−135.

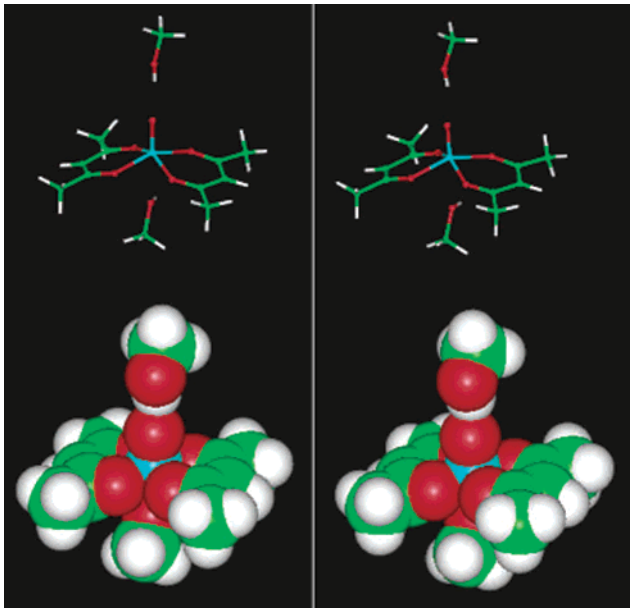

Figure 6. Stereo graphics model of the structure of $VO(acac)_2$ in solution constructed according to ENDOR constraints. The upper diagram illustrates the planar, *trans* conformation of the coordination complex with an axially bound solvent molecule coordinated to the vanadium atom and a solvent molecule hydrogen-bonded to the vanadyl oxygen, as detected by ENDOR. The lower diagram illustrates the complex in space-filling form, in the same projection as in the upper diagram. The atoms are color coded according to chemical element (C, green; O, red; H, white; V, cyan).

solution is illustrated in Figure 6 in space-filling and stick, skeletal image form.

In contrast to the equatorial, *trans* conformation of $VO(acac)_2$, detection by ENDOR of an axially positioned hydrogen in $VO(malto)_2$ that did not exchange with solvent indicated that the conformation of the VO^{2+} chelate in solution differed distinguishably from the X-ray structure. We note that the ENDOR spectra in Figure 5 together with EPR line width measurements required the presence of one equatorially coordinated methanol molecule. Also, the values of the EPR spectroscopic parameters of $VO(malto)_2$, namely, $g_{||}$ and $A_{||}$, remained consistent with an equatorial O_4 donor atom environment, according to the additivity relationships developed by Chasteen.[29] Therefore, a modeling search was carried out to identify a complex that simultaneously accounted for the ENDOR-detected axially positioned covalent hydrogen and the three types of equatorial organic hydrogens exhibiting vanadium−proton distances comparable to those in the crystalline complex. To this end, one maltolato ligand was kept unchanged from its X-ray-defined position while a search was carried out with the second maltolato ligand for a conformation that could yield a linear O═V···H configuration with a vanadium−H separation of 4.91 ± 0.25 Å.

This search was satisfied by bringing the second maltolato ligand into a *cis* conformation with respect to the ligand in the molecular *x*,*y* plane (cf. Figure 1) so that one oxygen donor atom occupied a coordination site in the equatorial plane while the second donor oxygen atom occupied an axial

(29) Chasteen, N. D. In *Biological Magnetic Resonance*; Berliner, L. J., Reuben, J., Eds.; Plenum: New York, 1981; Vol. 3, pp 53−119.

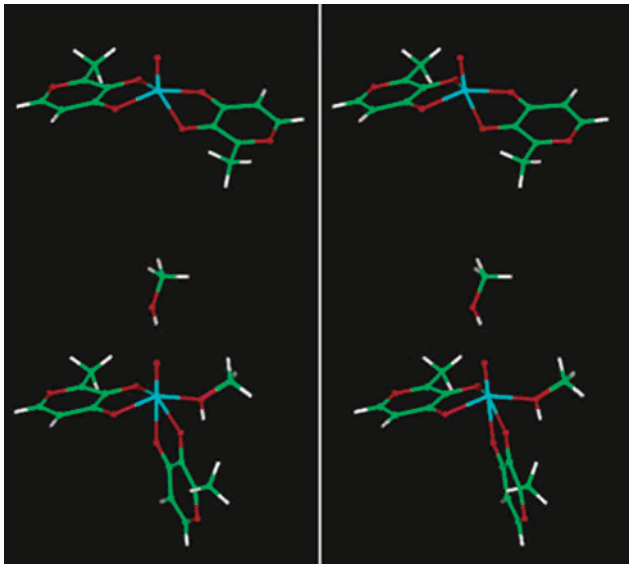

Figure 7. Stereo graphics model of the structure of $VO(malto)_2$ in solution constructed according to ENDOR constraints. The upper molecule illustrates the *trans*-$VO(malto)_2$ complex in crystals[7] for comparison. The lower molecule illustrates the structure of the *cis* complex in solution as defined through ENDOR with an equatorially coordinated methanol molecule. In the lower complex an axially positioned methanol molecule hydrogen-bonded with the vanadyl oxygen is also shown. The atoms are color coded according to chemical element as in Figure 6.

position below the plane opposite the vanadyl oxygen. This conformation positioned H5 of the *cis* ligand so that the angle subtended by O═V···H5 was 177° with a vanadium−H5 separation of 4.91 Å. Since the conformation of a *cis*-maltolato ligand with an axial methyl group resulted in a vanadium−H^{CH_3} separation of 5.40 Å, we concluded that the ENDOR-detected axial resonance in Figure 5 was best accounted for by the H5 proton. The hydroxyl group of a methanol molecule occupied the fourth equatorial coordination site to satisfy the EPR-detected decrease in line width of 1.25 ± 0.10 G upon introduction of $VO(malto)_2$ into perdeuterated methanol.[30] In addition to the equatorial methanol molecule, the ENDOR spectra provided evidence, as for $VO(acac)_2$, of an axially positioned methanol molecule hydrogen-bonded to the vanadyl oxygen.

The ENDOR-assigned *cis* conformation of $VO(malto)_2$ in solution is compared in Figure 7 to its X-ray structure. While ENDOR detection of an axial organic hydrogen demanded the presence of a *cis* conformer of the $VO(malto)_2$ complex, it is of interest to evaluate the extent to which a *trans* conformer may have also been present. Since the proton resonance features of an equatorial maltolato ligand in a *cis* complex would overlap with those in a *trans* complex, the distinction depends on detection of axial, inner-sphere-coordinated methanol in the *trans* complex. On the basis of earlier studies of the solvation structures of $[VO(CH_3OH)_4(H_2O)]^{2+}$ and $[VO(CH_3OH)_5]^{2+}$ (ref 13c), we concluded that the fraction of molecules populating the *trans* conformation

(30) Orvig and co-workers[8] have shown evidence on the basis of NMR studies for a *cis*-$[VO(malto)_2(CH_3O^-)]$ complex in which the central vanadium cation is diamagnetic, of oxidation state V, and equatorially coordinated to an ionized, methanol molecule. Our EPR and ENDOR results describe a neutral methanol molecule occupying the fourth, equatorial coordination site in a paramagnetic VO^{2+} complex.

must be ≤3−4% since no resonance features characteristic of axial, inner-sphere methanol were detected, in contrast to the results for $VO(acac)_2$ summarized in Table 1. This assessment is confirmed through measurement of the decrease in EPR line width of 1.25 ± 0.10 G for transfer of $VO(malto)_2$ into perdeuterated methanol. This value is quantitatively consistent with one equatorially coordinated hydroxyl proton at 100% occupancy of all paramagnetic sites in the sample.[25]

Because the V−O bond distance and O═V−O valence angle parameters of the equatorial oxygen atoms of the crystalline *trans*-$VO(malto)_2$ complex[8] are nearly identical to those in $VO(acac)_2$[7] and are sterically compatible with accommodating an axial methanol molecule, absence of an inner-sphere, axially coordinated solvent molecule in a *trans*-$VO(malto)_2$ complex could imply structural distortion preventing steric access to the vanadium cation. We consider such severe structural distortion unlikely.[31] We can only conclude that the population of *trans* conformers of the $VO(malto)_2$ complex in solution is below detection limits and is likely to be very small. We note in confirmation that Hanson et al. concluded from EPR spectra that the *cis* conformer of $VO(malto)_2$ in methanol and aqueous solutions was the dominant conformer.[32] On the basis of NMR and theoretical studies of the isomerization dynamics of diketonate-containing bis(chelate)dichlorovanadium(III) complexes being relevant, Rikkou and co-workers have pointed out that *cis* isomers are preferentially stabilized by polar solvents and that *trans* isomers are favored by high temperatures.[33] Since crystalline $VO(malto)_2$, having a *trans* conformation, is formed under refluxing conditions,[8] the higher temperature is possibly responsible for the *trans* conformation observed by X-ray crystallography.

E. *Cis*−*Trans* Conformational Equilibria of VO^{2+} Chelates. The variation of EPR spectra of $VO(acac)_2$[7b,34] and of $VO(malto)_2$[32] with pH or temperature has been ascribed to the presence of equilibrium mixtures of *cis* and *trans* conformers and of di- and hemichelated forms of the VO^{2+} ion. In previous studies, we quantified the fractional composition of EPR spectral species of $VO(acac)_2$ in solution as a function of pH.[3a] Three spectrally distinct species are formed in both aqueous and methanolic solutions with identical spectroscopic parameters. The ENDOR spectra of species formed at pH 3 and at pH 7 showed quantitatively neither a change in the stoichiometry of VO^{2+}-bound acetylacetonato ligand nor resonance features attributable to a *cis* conformation of the organic ligand. Thus, the ENDOR results provide no support for the interpretations of Crans and co-workers of conformational equilibria of $VO(acac)_2$.[7b,34] We conclude that the variation of EPR spectra of $VO(acac)_2$ with pH reflects only subtle changes in V−O covalency induced through small changes in displacement of the vanadium ion from the plane of the four equatorial donor oxygen atoms or alterations in O═V−O and V−O−C angle relationships. The *trans* conformation of $VO(acac)_2$ defined through ENDOR and illustrated in Figure 6 in general applies to all three spectral species formed in the pH range 2.5−7.0.[3a]

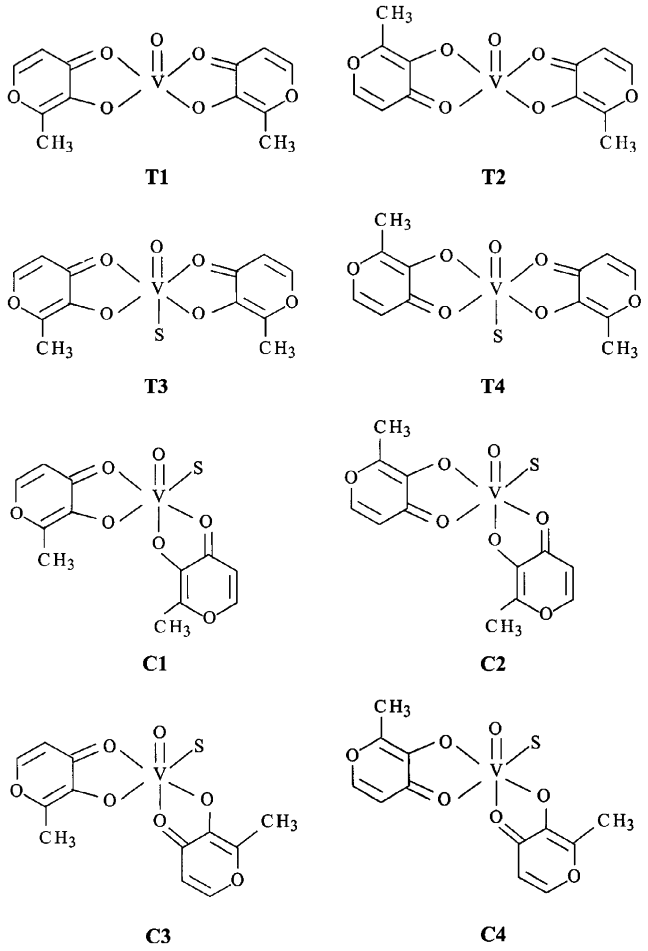

Figure 8. Diagrammatic illustration of possible conformational isomers of $VO(malto)_2$ in solution. See the text for discussion. S = solvent. Based on Hanson et al.[32]

Orvig and co-workers have similarly suggested that variations of EPR spectra of $VO(malto)_2$ with temperature in aqueous solution reflect *cis*/*trans* conformational equilibria and variation in the relative amounts of conformers with *syn* and *anti* orientations of the maltol ligand.[8,32] Eight species postulated by Hanson et al.[32] to account for variation of EPR spectra are illustrated in Figure 8. Only C3 and C4 as *cis* conformers are compatible with the ENDOR-determined electron−nucleus distances in Table 3, as discussed above. Although *syn* and *anti* conformers represented by species C3 and C4 are not distinguishable on the basis of ENDOR results, we believe that species C4 with an *anti* configuration is likely to be more highly populated. We note that the ground-state dipole arising from the distribution of electron

(31) Preliminary analysis of ENDOR spectra of bis(1-*N*-oxide-pyridine-2-thiolato)oxovanadium(IV)[1c] indicates no axially coordinated solvent although the organic ligands are equatorially positioned for the complex in solution (Mustafi, D.; Makinen, M. W. Unpublished observations). In this case, however, the van der Waals radii of equatorial sulfur donor atoms sterically prevent axial, inner-sphere coordination of solvent.

(32) Hanson, G. R.; Sun, Y.; Orvig, C. *Inorg. Chem.* **1996**, *35*, 6507.
(33) Rikkou, M.; Manos, M.; Tolis, E.; Sigalas, M. P.; Kabanos, T. A.; Keramidas, A. D. *Inorg. Chem.* **2003**, *42*, 4640.
(34) Crans, D. C. In *Vanadium Compounds: Chemistry, Biochemistry and Therapeutic Applications*; Tracey, A. S., Crans, D. C., Eds.; American Chemical Society Symposium Series No. 711, Oxford University Press: New York, 1998; pp 82−103.

density in the 4-pyrone ring will be oriented approximately parallel to the ether oxygen−keto oxygen axis. In the C3 species the two dipoles will be oriented approximately perpendicularly to each other, while in the C4 species they will be more nearly antiparallel. The latter will be associated with lower potential energy, and therefore, population of this isomer would be favored.

F. General Conclusions. This study has demonstrated the advantages of using VO^{2+} as an ENDOR probe for structural characterization of VO^{2+} chelates in solution. On the basis of X-ray crystallographic studies,[7,8] $VO(acac)_2$ and $VO(malto)_2$ exhibit approximate, square-pyramidal geometry with *trans* equatorially oriented organic ligands without axially coordinated solvent molecules. On the basis of ENDOR studies, the disposition of the organic ligands in the $VO(acac)_2$ complex in solution was found not to differ from that in crystals while the resonance features of axially bound solvent molecules coordinated to the metal ion and hydrogen-bonded to the vanadyl oxygen were readily identified and analyzed. In sharp contrast, only the *cis* conformer of the $VO(malto)_2$ complex in solution was detected by ENDOR, with the donor oxygen atoms of one maltolato ligand equatorially coordinated to the central VO^{2+} moiety while one of the donor oxygen atoms of the second ligand was axially located and the second donor oxygen atom occupied an equatorial position *trans* to the vanadyl oxygen. Although both VO^{2+} complexes exhibit insulin-mimetic activity in diabetic laboratory animals and whole cell systems,[1,3,5] only $VO(acac)_2$ exhibits insulin-enhancing action that is synergistic with insulin, potentiating the tyrosine phosphorylative activity of the insulin receptor.[3b] Since the different biological activities of these VO^{2+} complexes are presumably determined by their structures in solution, the results of this study provide a basis for beginning to explore differences in the structural basis of their interactions with macromolecular components of the insulin-signaling system.

Acknowledgment. This work was supported by grants from the National Institutes of Health (DK57599) and from the National Science Foundation (MCB-0092524). We thank Dr. K. H. Thompson and Professor C. Orvig of the University of British Columbia for providing crystalline bis(maltolato)oxovanadium(IV).

IC040120Y